IEEE Access
Multidisciplinary | Rapid Review | Open Access Journal

SPECIAL SECTION ON INDEX MODULATION TECHNIQUES
FOR NEXT-GENERATION WIRELESS NETWORKS

Received September 26, 2017, accepted October 14, 2017, date of publication October 17, 2017,
date of current version November 7, 2017.

*Digital Object Identifier 10.1109/ACCESS.2017.2763978*

**INVITED PAPER**

# State-of-the-Art Design of Index Modulation in the Space, Time, and Frequency Domains: Benefits and Fundamental Limitations

**SHINYA SUGIURA, (Senior Member, IEEE), TAKUMI ISHIHARA, (Student Member, IEEE), AND MIYU NAKAO, (Student Member, IEEE)**

Department of Computer and Information Sciences, Tokyo University of Agriculture and Technology, Kogani 184-8588, Japan (e-mail: sugiura@ieee.org).

Corresponding author: Shinya Sugiura (sugiura@ieee.org)

This work was supported by the Japan Society for the Promotion of Science KAKENHI under Grant 26709028, Grant 16KK0120, Grant 17H03259, and Grant 17K18871.

**ABSTRACT** In this paper, we provide a comprehensive review of diverse index modulation (IM) architectures that operate in the space, time, and frequency domains, as well as their related technologies. We clarify that several IM-specific characteristics have explicit advantages over those of the conventional bandwidth-efficient counterparts, such as spatial multiplexing, orthogonal frequency division multiplexing, and single-carrier frequency division multiple access, which have been widely employed in the current wireless standards. While, for the next-generation wireless systems, multiple performance requirements that conflict with each other have been imposed, IM schemes have the potential of satisfying part of the requirements, in addition to enhancing bandwidth efficiency. More specifically, we characterize operational scenarios and system settings that specifically benefit from IM schemes versus their non-IM counterparts while clarifying the fundamental limitations and the open issues for IM schemes that have not been sufficiently explored previously. Furthermore, we also present the rationale of the recent novel IM scheme that amalgamates the time-domain IM scheme and the concept of faster-than-Nyquist signaling and attains a rate enhancement together with a low peak-to-average power ratio.

**INDEX TERMS** Index modulation, faster-than-Nyquist signaling, differential spatial modulation, OFDM-IM, single-RF, space-shift keying, space-time shift keying, spatial modulation, subcarrier index modulation, time-domain single-carrier index modulation.

## I. INTRODUCTION

Index modulation (IM) [1]–[10] has attracted much attention as an emerging modulation concept and is characterized by sparse symbol mapping. More specifically, activating a subset of the legitimate symbol indices allows an IM transmitter to send additional information, beyond that of the traditional amplitude and phase shift keying (APSK) modulation scheme, such as phase-shift keying (PSK) and quadrature amplitude modulation (QAM) [11]. The dimensions invoked for IM include space [2], [3], [6], [12]–[14], time [2], [15]–[17], and frequency [7], [8], [18], as well as the combinations space-time [2], [19], [20] and space-time-frequency [4], [21], [22]. In addition, several related IM techniques, including ones based on beamspace [23], [24] and distributed-node space [25]–[27], have been developed.[1] In contrast to the classic full-symbol-allocation frameworks that provide high bandwidth efficiencies and high peak data rates, IM-based sparse symbol mapping schemes are capable of providing different advantages under specific useful scenarios, as highlighted throughout this paper.

Conventional modems are designed to allocate as many symbols as possible to each dimension while maintaining

[1] In this paper, we focus our attention on a review of non-distributed IM techniques in multiple dimensions. For further details of distributed spatial modulation, refer to [2], [3], [28] and references therein.

**TABLE 1. Multiplexing versus index modulation in each domain.**

| Dimension | Multiplexing (Full allocation) | Index modulation (Sparse allocation) |
|---|---|---|
| Space | Spatial multiplexing | Spatial modulation |
| Frequency | OFDM | OFDM-IM (SIM) |
| Time | SC/FDMA | SCIM/FDMA |

their orthogonality in order to increase the bandwidth efficiency and peak data rate. For example, in the spatial multiplexing multiple-input multiple-output (MIMO) arrangement [29]–[32], a transmitter sends independent parallel symbol streams from multiple transmit antenna elements, hence enabling symbol multiplexing in the spatial domain. In spatial multiplexing, the transmission rate linearly increases with the minimum of the numbers of transmit and receive antenna elements, and this is achieved without expanding the bandwidth. Furthermore, in orthogonal frequency division multiplexing (OFDM) [11], [33], [34], a serial data stream is serial-to-parallel (S/P) converted into a number of low-rate parallel streams that are modulated onto multiple orthogonal subcarriers in the frequency domain. The symbols modulated onto the orthogonal subcarriers are then combined to form an OFDM frame with the aid of an inverse discrete fast Fourier transform (IDFT). An explicit benefit of OFDM is that robustness over multipath propagation, as well as the mitigation of inter-symbol interference (ISI), is achieved while allowing discrete fast Fourier transform (DFT)-assisted low-complexity detection at the receiver. As one close relative of OFDM, single-carrier (SC) symbol transmissions in frequency-division multiple access (FDMA) used with frequency-domain equalization (FDE) [35], [36] constitute the time-domain counterpart of OFDM while achieving a significantly lower peak-to-average power ratio (PAPR) than OFDM. Note that the system models of OFDM and SC/FDMA-FDE are essentially the same, except that both the DFT and IDFT are incorporated into the receiver in the SC/FDMA-FDE system, while the IDFT and DFT are used at the transmitter and receiver, respectively, in the OFDM system [36]. These three representative orthogonal full-symbol-allocation frameworks, spatial multiplexing, OFDM, and SC/FDMA-FDE (listed in Table 1), have been widely employed in the current broadband wireless standards [37], [38].

IM schemes in the space, frequency, and time domains were developed as spatial modulation [3], OFDM-IM [7], and SC-based IM (SCIM)/FDMA [15], and are the IM counterparts of spatial multiplexing, OFDM, and SC/FDMA, as shown in Table 1. Importantly, when targeting an ultimate increase of bandwidth efficiency, the above-mentioned conventional full-allocation schemes may outperform the IM schemes. However, the next-generation wireless systems have several performance requirements imposed on them that conflict with each other, in terms of not only the peak data rate but also the latency, reliability, traceability, energy efficiency, and number of connections [39], [40]. To this end, in this paper we focus our attention on the metrics, such as the tradeoff between energy and bandwidth efficiencies, as well as the latency in low-rate multiple access, wherein the benefits of IM over the conventional frameworks become explicit. Naturally, these benefits may be achieved at the cost of several specific disadvantages that have to be carefully avoided when adopting IM.

Against this background, the main contributions of this paper over previous IM-related tutorials [1]–[10] are as follows.

- We review and classify the IM family in the space, time, and frequency domains in a comprehensive manner. This is done with the aim of guiding the reader to scenarios beneficial for IM schemes, since the IM-specific merits are different from those of the conventional full-allocation frameworks, such as spatial multiplexing, OFDM, and SC/FDMA.
- Since the benefits of the IM family are attained with the imposition of several fundamental limitations, we clarify these fundamental limitations, which have previously been insufficiently explored, including those of SC transmissions and time-limited pulse shaping for single-RF spatial modulation, as well as those of low-rate regions beneficial for OFDM/IM and SCIM/FDMA.
- Until recently, time-domain IM schemes have not been investigated as exhaustively as their space- and frequency-domain counterparts. Therefore, we first highlight and review the latest results in time-domain IM schemes, such as SCIM and faster-than-Nyquist (FTN)-IM, which have the merits of a rate enhancement and a low PAPR.

The remainder of this paper is organized as follows. We review the IM family in the spatial domain in Section II. In Section III, the IM incorporating both the space and time domains is described. Furthermore, IM schemes exploiting the frequency and time domains are introduced in Sections IV and V, respectively. Then we lay out the challenges and future directions of IM in Section VI, before finally concluding this paper with Section VII.

## II. SPATIAL MODULATION: IM IN THE SPATIAL DOMAIN

In this section, we introduce the basic principles, benefits, and limitations of the IM family that operates in the spatial domain. Chau and Yu [41] proposed the original concept of spatial modulation, in which the transmitter supports multiple antenna elements and the combination of activated transmit antenna elements per symbol interval conveys information bits, although multiple RF chains are needed in their arrangement. Haas *et al.* [42] modified the modulation principle of [41] to one relying on the activation of only a single transmit antenna element in each symbol interval, hence enabling a single-RF transmitter structure. As a result, low cost and high energy efficiency, which are benefits specific to spatial modulation, are attained.

Under the idealized assumptions of SC symbol transmissions over a frequency-flat fading channel, the received signals $\mathbf{y}_s \in \mathbb{C}^{N_{\rm rx}}$ (where $N_{\rm rx}$ is the number of receive antenna elements; note, $N_{\rm tx}$ is the number of transmit antenna elements), of each time instance are given by

$$\mathbf{y}_s = \mathbf{H}_s\mathbf{s}_s + \mathbf{n}, \tag{1}$$
$$= s_s\mathbf{h}_s^{(l)} + \mathbf{n}. \tag{2}$$

The symbol vector $\mathbf{s}_s \in \mathbb{C}^{N_{\rm tx}}$ contains only a single non-zero APSK-modulated symbol $s_s \in \mathbb{C}$ in the activated $l$th antenna element and the other $N_{\rm tx}-1$ elements in $\mathbf{s}_s$ are zeros:

$$\mathbf{s}_s = [0\cdots 0\, s_s\, 0\cdots 0]^T, \tag{3}$$
$$\uparrow$$
$$\text{the } l\text{th element}$$

where $[\cdot]^T$ denotes the transpose operation. The constructed sparse symbol vector of (3) is in contrast with the symbol vector of the conventional spatial multiplexing scheme, which is filled with $N_{\rm tx}$ symbols. Furthermore, $\mathbf{H}_s = \left[\mathbf{h}_s^{(1)}\cdots\mathbf{h}_s^{(N_{\rm tx})}\right] \in \mathbb{C}^{N_{\rm rx}\times N_{\rm tx}}$ is the complex-valued channel matrix, and $\mathbf{n} \in \mathbb{C}^{N_{\rm rx}}$ are the associated AWGN components, which are given by random variables obeying the complex-valued Gaussian distribution $\mathcal{CN}(0, N_0)$, that is, the distribution having a mean of zero and a variance of $N_0$. In each symbol interval, both the index of an activated transmit antenna element $l$ ($0 \le l \le N_{\rm tx}$) and the symbol $s_s$ modulated with the aid of $\mathcal{M}$-point APSK convey information bits to the receiver.[2] Hence, the transmission rate of spatial modulation is

$$R_{\rm SM} = \log_2 N_{\rm tx} + \log_2 \mathcal{M} \quad \text{[bits/symbol]}. \tag{4}$$

From (4), spatial modulation has scalability in terms of transmit antenna elements: its transmission rate $R_{\rm SM}$ logarithmically increases with an increase in the number of transmit antenna elements $N_{\rm tx}$.[3] Note that spatial multiplexing linearly increases the transmission rate $R_{\rm SMX}$, which is given by

$$R_{\rm SMX} = N_{\rm tx}\log_2 \mathcal{M} \quad \text{[bps/Hz]}, \tag{5}$$

although it requires a full-RF transmitter structure.

Fig. 1 compares the transmitter structures of spatial modulation and spatial multiplexing for the case of considering $N_{\rm tx} = 4$ transmit antenna elements. As shown in Fig. 1(a), the spatial modulation transmitter activates only one of the four transmit antennas in each symbol interval, which conveys $\log_2 N_{\rm tx} = 2$ IM bits, in addition to the $\log_2 \mathcal{M}$ modulated bits. Owing to the antenna switching mechanism of spatial modulation, each symbol duration has to be less than or equal to the symbol interval, as shown in Fig. 1(a), although the full-RF spatial multiplexing transmitter of Fig. 1(b) does not have this limitation, similar to other modems.

Bearing in mind that the classic full-RF spatial multiplexing transmitter is equipped with the same number of RF chains as the number of transmit antenna elements $N_{\rm tx}$, the main benefits of the single-RF spatial modulation transmitter can be classified into low detection complexity, low terminal and calibration costs, low energy consumption, and an open-loop architecture, which are explained in brief as follows:

1) **Low decoding complexity:** Since the spatial modulation transmitter sends only a single symbol in each symbol interval rather than relying on symbol multiplexing, its receiver does not have to decouple multiple streams, while that of spatial multiplexing does. Optimal maximum likelihood (ML) detection was presented for spatial modulation in [13] and may benefit from a single-stream-based low detection complexity, increasing exponentially with an increase of the transmission rate given by (4). More sophisticated detection algorithms, based on matched filtering [47] and sphere decoding [48], were developed for attaining a significantly lower decoding complexity than their ML counterpart. The two-stage detection of [47] was further improved in [49] and [50]. Note that a detailed discussion of spatial modulation detectors may be found in [32]. Furthermore, while most previous spatial modulation detection algorithms were developed in the context of frequency-flat (narrowband) channels, in [51] and [46] reduced-complexity time-domain equalization (TDE) and FDE were developed for broadband SC spatial modulation scenarios.
2) **Low terminal and calibration cost:** The single-RF structure of the spatial modulation contributes to a simplification of the transmitter. Since in general each RF chain typically contains a digital-to-analog (D/A) converter, a mixer, a filter, and a power amplifier, as well as other elements, the associated cost of single-RF spatial modulation is one-$N_{\rm tx}$th that of full-RF spatial multiplexing. Additionally, the single-RF spatial modulation transmitter does not require calibration of multiple RF chains, unlike a conventional full-RF MIMO transmitter. These characteristics are beneficial not only for a base station, having a large number of antenna elements, but also for a mobile handset, because such handsets typically are severely constrained with respect to the terminal size and cost, as well as energy efficiency.
3) **Low energy consumption:** The conventional full-RF MIMO transmitter suffers from high energy consumption, which is caused by the need to have multiple RF chains [3], [52]. To be more specific, in addition to

[2] A rule employed for mapping information bits onto a symbol vector affects the achievable performance of the SM scheme. In [43], the bit-to-symbol mapper, which maximizes constrained information rate of the SM scheme, was proposed. Furthermore, Yang *et al.* [44] presented bit-to-symbol mapping rule for the SM scheme, which increases hamming distance between SM symbols. Also, in [45], the SM scheme's bit-to-symbol mapping rule was developed, by assuming a scenario where partial knowledge of channel state information (CSI) is available at the transmitter.

[3] Since single-RF spatial modulation does not support bandwidth-efficient time-orthogonal pulse shaping [46], the units of (4) are bits/symbol rather than bps/Hz. A detailed discussion will be provided in Section VI-A.

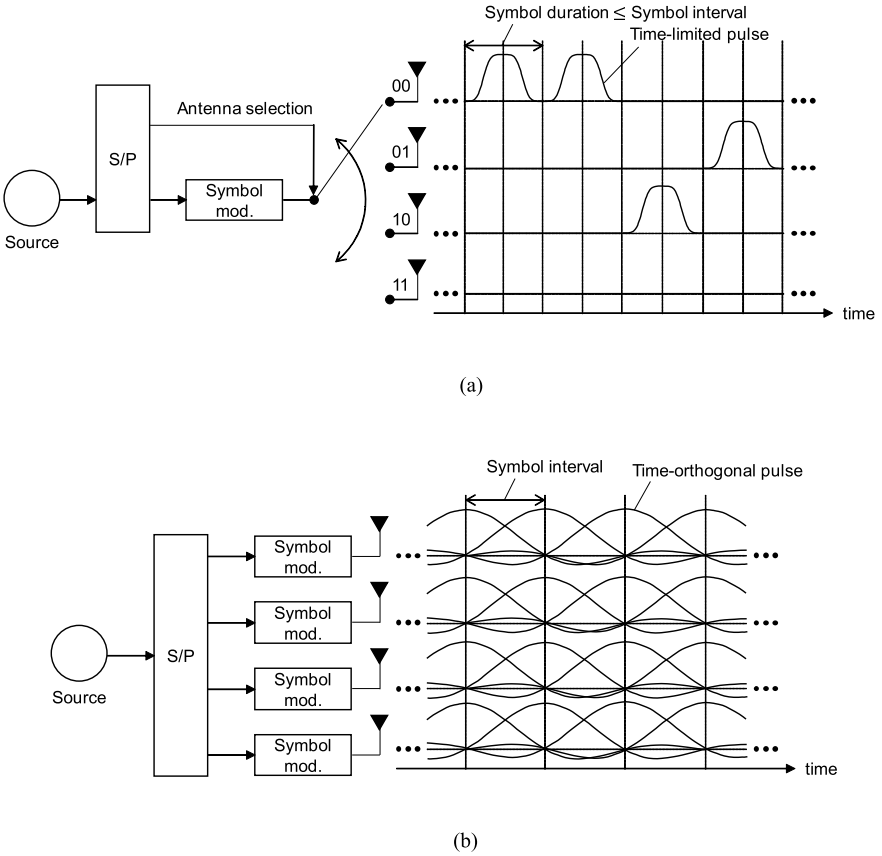


**FIGURE 1.** Transmitter structures: (a) single-RF spatial modulation and (b) full-RF spatial multiplexing.

the dynamic RF power consumption, the static power consumption imposed by the circuit (e.g., the power amplifier) linearly increases with the number of transmit antenna elements in the conventional full-RF MIMO transmitter. Note that, as mentioned in [3], it has recently been revealed that full-RF MIMO systems may be less energy-efficient than their single-antenna counterparts when both the dynamic and static power consumptions are considered in a fair manner. This is obvious for the massive-MIMO scenario, where a high number of transmit antenna elements are used at the base station. However, single-RF spatial modulation is capable of maintaining a low energy consumption even upon increasing the number of transmit antenna elements. Hence, in single-RF spatial modulation, the energy consumption at the peak data rate tends to be significantly lower than that in full-RF spatial multiplexing [52]. Note also that a high energy efficiency at the base station is an important requirement for next-generation cellular systems [53].

4) **Open-loop operation:** Additionally, the spatial modulation system does not assume CSI at the transmitter (CSIT). This allows us to avoid the use of a feedback channel, which consumes additional bandwidth while increasing latency. Hence, this benefit is most obvious for a scenario where a mobile terminal is moving quickly. Note that while optional closed-loop spatial modulation schemes, such as those relying on adaptive antenna selection [54]–[56], precoding [57], [58], and beamforming [59], have been proposed, they are not the main focus of this paper.

The above-mentioned benefits exclusive to spatial modulation are achieved at the expense of accepting specific limitations, which may not have been taken into account typically in the early and even in many recent studies on spatial modulation. The two main ones are highlighted below.

1) **Single-carrier limitation:** A recent study [46] revealed that a single-RF spatial modulation system has to employ SC symbol transmissions rather than multicarrier ones. This is because antenna activation in each subcarrier of OFDM would result in simultaneous activation of multiple antenna elements, hence requiring multiple RF chains.
2) **Time-limited pulse shaping:** As clarified in [60], a single-RF spatial modulation transmitter has to employ time-limited pulse shaping, since a whole symbol has to be transmitted during the activated symbol interval, as shown in Fig. 1(a). This implies that a

**TABLE 2. Classification of index modulation schemes.**

| Dimension | Scheme | # of RF | CSIR | Carriers | Shaping filter | Target |
|---|---|---|---|---|---|---|
| Space | Spatial modulation [12] | Single | Exact | Single-carrier | Time-limited | Rate/Cost/Energy |
| | Generalized spatial modulation [61] | Multiple | Exact | Single-carrier | Time-limited | Rate/Cost/Energy |
| | Space-shift keying [14] | Single | Exact | Single-carrier | Time-limited | Rate/Cost/Energy |
| | Semi-blind spatial modulation [62] | Single | Semi-blind | Single-carrier | Time-limited | Rate/Cost/Energy |
| | Rectangular DSM [63] | Single | Semi-blind | Single-carrier | Time-limited | Rate/Cost/Energy |
| | Quadrature spatial modulation [64] | Single | Exact | Single-carrier | Time-limited | Rate/Cost/Energy |
| Space-time | STSK [19] | Full | Exact | No limitation | No limitation | Rate/Reliability |
| | Asynchronous STSK [19] | Single | Exact | Single-carrier | Time-limited | Rate/Reliability/Cost/Energy |
| | Generalized STSK [20] | Full | Exact | No limitation | No limitation | Rate/Reliability |
| | DSTSK [19] | Full | Unneeded | No limitation | No limitation | Low-rate reliability |
| | DSM [65, 66] | Single | Unneeded | Single-carrier | Time-limited | Low-rate reliability/Cost/Energy |
| Beamspace | Beamspace IM [23] | Single | Exact | Single-Carrier | Time-limited | Rate/Cost/Energy |
| | Reconfigurable spatial modulation [24] | Single | Exact | Single-Carrier | Time-limited | Rate/Reliability/Cost/Energy |
| | Reconfigurable DSM [24] | Single | Unneeded | Single-Carrier | Time-limited | Low-rate reliability/Cost/Energy |
| Code | Parallel combinatory SS [67] | – | Exact | Single-carrier | No limitation | Low-rate performance |
| | Parallel combinatory FHSS [68] | – | No need | Multi-carrier | No limitation | Low-rate performance |
| Frequency | OFDM-IM (SIM) [18] | – | Exact | Multi-carrier | No limitation | Low-rate performance |
| | Dual-mode OFDM-IM [69] | – | Exact | Multi-carrier | No limitation | Low-rate performance |
| Time | PPM [70] | – | Exact | No limitation | No limitation | Low-rate performance |
| | SCIM [15] | – | Exact | Single-carrier | No limitation | Low-rate performance |
| | Dual-mode SCIM [17] | – | Exact | Single-carrier | No limitation | Low-rate performance |
| | FTN-IM [16] | – | Exact | Single-carrier | No limitation | Low-rate performance |
| Space-time | STFSK [21] | Full | Exact | Single-carrier | No limitation | Rate/Reliability |
| -frequency | OFDMA/SC-FDMA-aided STSK [22] | Full | Exact | No limitation | No limitation | Rate/Reliability |
| Distributed | Cooperative DF STSK [25] | Single | Exact | No limitation | No limitation | Rate/Reliability |
| (Cooperative) | Cooperative DF DSTSK [25] | Single | Unneeded | No limitation | No limitation | Low-rate reliability |
| | Single-relay AF SSK [26] | Single | Exact | Single-carrier | Time-limited | Rate/Cost/Energy |

bandwidth-efficient shaping filter, such as a root raised cosine (RRC) filter, is not applicable for single-RF spatial modulation. The associated performance penalty is not imposed on other conventional full-RF MIMO transmitters.

These two limitations will be further detailed in Section VI, which also provides their partial solutions and future directions.

In the rest of this section, we introduce several related spatial modulation techniques that rely on the IM principle in the spatial domain. The diverse possible IM arrangements, including those reviewed in Sections II–V, are compared in Table 2.

### A. MULTIPLE-RF GENERALIZED SPATIAL MODULATION

The original spatial modulation scheme activates only a single transmit antenna element in each symbol interval, and hence information bits conveyed by IM is limited in comparison to the full-RF spatial multiplexing scheme, as seen in the relationship between (4) and (5). To this end, multiple-RF generalized spatial modulation (GSM) [61], [71] was proposed, in which multiple transmit antenna elements are activated during each symbol interval and multiple symbols are simultaneously transmitted from different transmit antenna elements in a similar manner to spatial multiplexing. This change implies that GSM is capable of striking a flexible balance between the reduced number of RF chains of spatial modulation and the high peak data rate of spatial multiplexing. Naturally, when the number of RF chains is less than the number of transmit antenna elements, the GSM system still has the limitations of SC transmissions and time-limited pulse shaping, similar to single-RF spatial modulation.

### B. BEAMSPACE (RECONFIGURABLE) INDEX MODULATION

In spatial modulation, in order for the receiver to classify an activated antenna index in a stable way, the channel

correlations associated with transmit antenna indices have to be as low as possible. Hence, sufficient separations between the transmit antenna elements are needed, similar to the classic MIMO systems [72]. In order to satisfy the requirement of low channel correlations, the transmitter size may become large, especially when the operating frequency is as low as that of microwaves, rather than those of millimeter waves and visible light. To this end, the concept of beamspace (reconfigurable) IM was developed in [9], [23], and [24]. Beamspace IM becomes realistic with the aid of pattern-reconfigurable active and/or switched antenna devices [73]–[76]. More specifically, instead of exploiting transmit antenna indices as used in spatial modulation, the activation of only one of the multiple antenna patterns conveys IM bits to the receiver. The merit of beamspace IM is that the size of a reconfigurable antenna device is fixed, regardless of the number of antenna patterns, while the size of an antenna unit in spatial modulation becomes higher upon increasing the number of transmit antenna indices.

However, in beamspace IM, upon increasing the number of legitimate antenna patterns, the channel correlations associated with the antenna patterns increase. This implies that beamspace IM has a tradeoff between the code rate and the achievable performance. Recently, the effects of channel correlation on the performance of beamspace IM were studied in [77] by considering Rician fading channels. However, since the effects of channel correlation largely depend on the types of active antennas, investigations that consider more specific antenna devices are left for future studies. Moreover, similar to other single-RF spatial modulation schemes, beamspace IM has limitations associated with SC and time-limited pulse shaping, when assuming the use of a single-RF transmitter.

### C. SEMI-BLIND SPATIAL MODULATION

In spatial modulation, the acquisition of CSI at the receiver (CSIR) is typically assumed for symbol detection. The CSIR is available by periodic transmissions of pilot (training) symbols from the transmitter, as well as by CSI estimation at the receiver. However, upon increasing the number of transmit antenna elements, the pilot overhead, as well as the processing complexity required for CSI estimation, substantially increases. Although the use of a large-scale antenna array is needed for a high-rate spatial modulation, this limitation becomes more realistic.

In order to reduce the effects of pilot overhead, it may be possible to employ semi-blind detection as presented in [62] and [63], where semi-blind joint channel estimation and data detection were developed for spatial modulation. The CSI estimated with the aid of received pilot signals is used for initial symbol detection, and then the detected symbols are used as a long pilot sequence in order to improve the accuracy of channel estimation. CSI estimation and symbol detection are repeated until convergence. As the explicit benefit of this iterative gain, pilot overhead required for spatial modulation is reduced to the minimum.

### D. SPATIAL-MODULATION-BASED MASSIVE-MIMO DOWNLINK

As mentioned above, the benefit of spatial modulation is obvious when the number of transmit antenna elements is significantly high, since the number of RF chains is maintained at one at the transmitter, regardless of the number of transmit antenna elements. In the next-generation wireless systems, it is expected that the massive MIMO technique [78]–[80] will play an important role for further enhancing the spectral efficiency. More specifically, in the representative conjugate-beamforming massive MIMO downlink [78], the availability of CSIT is assumed in order to concentrate the transmit power on each receiver, hence allowing a significantly high RF energy efficiency. However, as mentioned above, the static circuit power consumption of this full-RF massive MIMO is very high, due to the massive number of RF chains. Furthermore, the need for CSIT imposes an additional feedback channel and/or the use of a time-division duplex (TDD). By contrast, spatial modulation typically is used in an open-loop system that only requires CSIR rather than CSIT, and hence is capable of dispensing with the associated overhead and feedback channel. Because of the absence of beamforming, the energy efficiency of RF power transmissions in spatial modulation may be lower than with the conjugate-beamforming massive MIMO scheme [78] . However, introducing analog beamforming into the spatial modulation transmitter may further enhance the dynamic RF energy efficiency, as shown in [81].

### E. OTHER APPLICATIONS OF SM

Non-orthogonal multiple access (NOMA), based on non-linear processing, constitutes one of the promising techniques for the next-generation wireless systems [82]. In comparison to the traditional orthogonal multiple access counterpart, the NOMA system is characterized by allocating each user in the power domain, while using the same time, space, and frequency resources. Furthermore, the use of MIMO in NOMA scenarios has attracted much interest [83]. In [84], the NOMA concept was introduced into an SM-assisted multiuser downlink scenario, which allows us to attain a high spectrum efficiency. In [85], the SM-assisted NOMA scheme was developed in the context of vehicle-to-vehicle communication systems, in order to deal with the detrimental effects of wireless vehicular channels. In [86], the achievable spectrum efficiency of the SM-aided NOMA downlink was investigated by deriving an accurate approximation of mutual information.

Moreover, in [87]–[89] the SM principle was introduced into cognitive radio system, which utilizes spectrum sharing [90]. The detailed survey of the SM-aided cognitive radio is found in [10].

## III. IM IN THE SPACE AND TIME DIMENSIONS

In this section, we introduce the IM family that exploits both the space and time domains, such as coherent space-time IM

and differential spatial modulation (DSM). Note that in these schemes, the time domain is exploited to attain a diversity gain, rather than increasing the transmission rate.

### A. SPACE-TIME IM

The original spatial modulation of Section II relies on IM only in the spatial domain. In order to include both the space and time dimensions in the symbol activation of IM, a space-time IM scheme, referred to as space-time shift keying (STSK), was created in [19]. In STSK, only one of the multiple space-time dispersion matrices is activated during each block interval. The STSK scheme is capable of striking a flexible tradeoff between the code rate and the diversity gain. This was achieved by carefully designing the size and elements of the dispersion matrices [19], [91].[4] Note that although the basic STSK transmitter requires a full-RF structure, the STSK scheme is also capable of operating in a single-RF transmitter arrangement if a sparsity is imposed on the design of space-time dispersion matrices, in which case the scheme is referred to as asynchronous STSK (ASTSK) [19]. Since the STSK scheme subsumes the SM scheme [2], the reduced-complexity detection algorithms developed for either scheme [47]–[50], [92], [93] are readily exchangeable. Moreover, several similar space-time IM schemes were developed independently to attain the same benefits, for example, those in [94] and [95].

In [20], STSK was further extended to generalized STSK (GSTSK), which activates multiple dispersion matrices during each block interval. This unified GSTSK framework subsumes diverse conventional MIMO arrangements, such as spatial multiplexing [96], orthogonal space-time block coding (OSTBC) [97], [98], spatial modulation [42], space-shift keying [14], STSK [19], GSM [61], and spatial modulated STBC [99], as shown in [20] and [2].

### B. DIFFERENTIAL SPATIAL MODULATION

Spatial modulation has the merit of linearly increasing the transmission rate with an exponential increase of the number of transmit antennas while maintaining a single-RF transmitter structure. However, the increase in code rate is achieved under the assumption of the ideal situation that all the associated CSI are precisely acquired at the receiver. Practically, the periodic insertion of pilot symbols is needed, which may result in significantly high overhead for the scenario of a high number of transmit antenna elements.

In order to dispense with the pilot overhead imposed on (coherent) spatial modulation, its non-coherently detected DSM counterpart is adopted with the aid of the classic unitary differential space-time modulation (UDSTM) concept [65], [66]. At the UDSTM transmitter, unitary matrices are differentially encoded in order to generate the unitary matrix for transmission. This allows the receiver counterpart of the transmitter to detect each block in a non-coherent manner, specifically, by differentially decoding two successive received signal blocks. Full diversity gain is achieved without requiring any CSI estimation at the receiver.

The single-RF DSM scheme is realized by UDSTM by means of constraining the unitary matrices of UDSTM to be sparse, specifically, such that each column contains only a single non-zero element. Note that the main target of DSM is the achievement of a transmit diversity gain rather than an increase in the code rate. This implies that the coherently detected counterpart of DSM is the space-time IM of Section III-A rather than the spatial modulation of Section II.

As mentioned above, the original single-RF DSM was presented in [65] and [66], in which the unitary group codes were designed to have sparse matrix structures, but the benefit of a single RF transmitter was not the focus of those studies. In [100], the design of the sparse unitary matrices of DSM was further investigated with the aid of cyclic algebras. In [25] and [101], motivated by the development of single-RF spatial modulation, the benefits of signal-RF DSM were discussed. Furthermore, several design methods of unitary matrices for single-RF DSM were presented in [102]–[107], which share a framework relying on sparse UDSTM. Also, in [108], the single-RF DSM transmitter structure was relaxed to include multiple RF chains, so as to improve the coding gain. In [109], a single-RF DSM was modified for supporting time-dimension and orthogonal in-phase and quadrature spatial dimensions, which is referred to as differential quadrature SM. However, all the above-mentioned single-RF DSM family rely on the use of unitary matrices.

The main limitations of DSM are that 1) it is not scalable with respect to the number of transmit antenna elements, and that 2) it only operates under the narrowband scenario. Detailed discussions of two these disadvantages will be given later in Sections VI-C and VI-D. In addition, the limitations of SC transmissions and time-limited pulse shaping in single-RF spatial modulation are also present in single-RF DSM.

In order to combat the above-mentioned scalability limitation in terms of the number of transmit antennas, which is due to the square unitary matrices used for DSM, rectangular DSM (RDSM) was proposed in [63]. In rectangular DSM, the differentially encoded unitary matrix of DSM is projected onto a rectangular matrix before transmission, which allows the number of symbol intervals needed for each block transmission to be decreased, hence resulting in an increased throughput in comparison to conventional DSM schemes. However, at the RDSM receiver, the $n$th block in a frame is detected with the aid of all the previous $n-1$ detected blocks together with an $N_{\rm tx}$-length initial pilot block, while the conventional DSM receiver is capable of carrying out error-propagation-free non-coherent detection based on only two successive received blocks.

[4] Alternatively, it may be possible to jointly optimize the constellation and the dispersion matrices so as to maximize constrained mutual information [43].

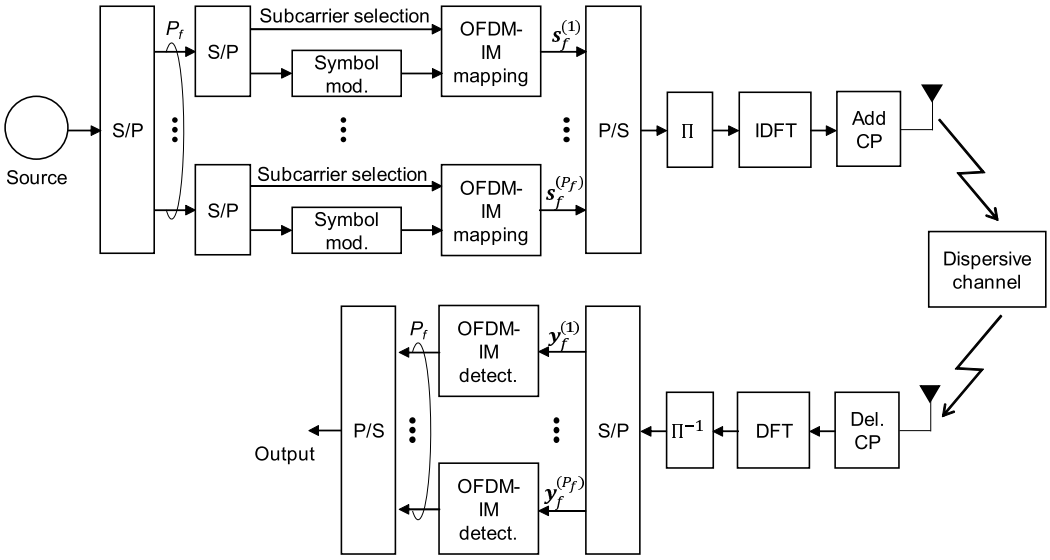


(a)

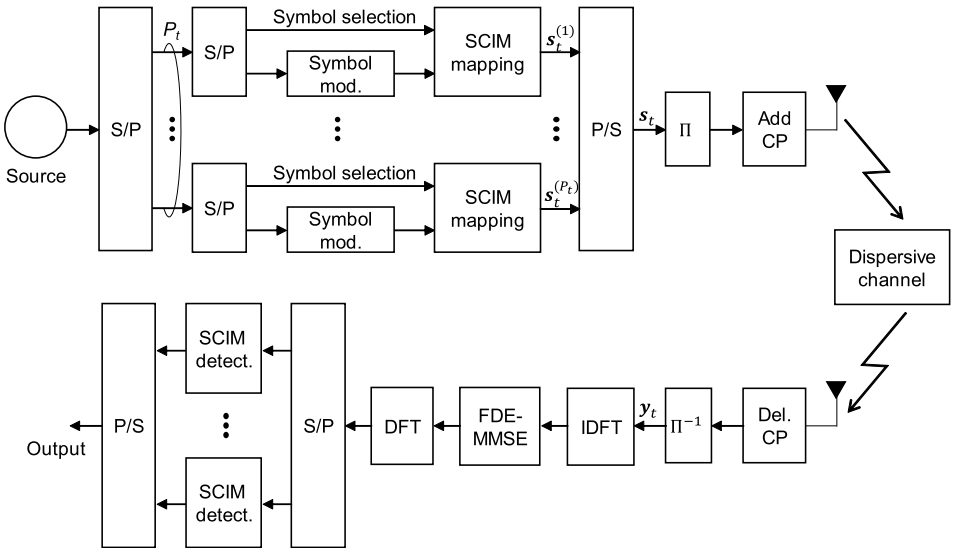


(b)

**FIGURE 2.** Transceiver structures: (a) OFDM-IM and (b) SCIM.

## IV. OFDM WITH SUBCARRIER INDEX MODULATION: IM IN THE FREQUENCY DIMENSION

OFDM-IM is the IM scheme using the frequency domain, which was originally proposed as parallel combinatory OFDM in [18]. Fig. 2(a) portrays the transceiver structure of OFDM-IM. The $N_f$ subcarriers are grouped into $P_f$ sets of $M_f$ subcarriers, such that $N_f = P_f M_f$. In each subcarrier set, $K_f$ out of the $M_f$ subcarriers are activated per OFDM-IM frame, while $K_f$ of the $\mathcal{M}$-point APSK symbols are modulated onto the activated subcarriers and the other $M_f - K_f$ subcarriers are deactivated. Here, the frequency-domain symbols are $\mathbf{s}_f^{(p)} \in \mathbb{C}^{M_f}$ $(p = 1, \cdots, P_f)$ for the $p$th subcarrier set. In OFDM-IM, the combination of the activated subcarrier indices together with the $K_f$ APSK-modulated symbols convey information bits.

The $N_f$ symbols $\mathbf{s}_f = [\mathbf{s}_f^{(1)T}, \cdots, \mathbf{s}_f^{(P_f)T}]^T \in \mathbb{C}^{N_f}$ in the frequency domain are interleaved by $\Pi$. Then, by carrying out an IDFT over the $N_f$ interleaved subcarriers, we arrive at the time-domain OFDM-IM frame, which is transmitted after adding a cyclic prefix (CP).

At the receiver, the CP is removed from the time-domain received signals, and then a DFT is performed to obtain

the frequency-domain signals. After deinterleaving them by $\Pi^{-1}$, the frequency-domain signals $\mathbf{y}_f^{(p)} \in \mathbb{C}^{M_f}$ associated with the $p$th OFDM-IM subcarrier set are obtained by

$$\mathbf{y}_f^{(p)} = \mathbf{H}_f^{(p)} \mathbf{s}_f^{(p)} + \mathbf{n}, \tag{6}$$

where $\mathbf{H}_f^{(p)} \in \mathbb{C}^{M_f \times M_f}$ denotes the frequency-domain channel transfer matrix for the $p$th subcarrier set. Note that when there is no inter-subcarrier correlation, the frequency-domain channel transfer matrix $\mathbf{H}_f^{(p)}$ is diagonal. The normalized throughput of OFDM-IM is given by [7]

$$R_{\text{OFDM-IM}} = \frac{K_f \log_2 \mathcal{M} + \left\lfloor \log_2 \binom{M_f}{K_f} \right\rfloor}{M_f} \quad \text{[bps/Hz]}, \tag{7}$$

The rate $R_{\text{OFDM-IM}}$ of (7) does not include the penalty imposed by the CP insertion for the sake of simplicity. The first term of (7) corresponds to information bits modulated onto the classic APSK modulation scheme, while the second term represents those sent with the aid of the activated subcarrier indices.

At the receiver, the indices of activated subcarriers and the modulated symbols are detected using (6). An exhaustive ML search achieves the best attainable performance. However, when the search space associated with IM, i.e., $\binom{M_f}{K_f}$, is large, the ML detection becomes infeasible, due to an excessively high search complexity. In order to reduce the detection complexity, the low-complexity suboptimal detection algorithm, which is referred to as log-likelihood ratio (LLR) detection [110], was developed; the resultant complexity is almost as low as that of OFDM.

In order to improve its effective transmission rate, in [111] the OFDM-IM was generalized to be capable of accepting varying numbers of active subcarriers contained in the subcarrier sets. Furthermore, in [111], the indices of in-phase and quadrature-phase per subcarrier were independently mapped in order to increase spectral efficiency. Also, a dual-mode OFDM scheme was proposed in [69] which uses a combination of two constellation modes, rather than a single constellation mode and zero symbols.

Against the above-mentioned beneficial characteristics, fundamental limitations are imposed on the OFDM-IM scheme, which are highlighted as follows.

1) **High PAPR:** Although the activated subcarriers in OFDM-IM may be sparse in comparison to those of OFDM, the OFDM-IM and OFDM schemes typically suffer from a similar high-PAPR profile, as mentioned in [7]. More specifically, the maximum PAPR value of OFDM-IM may be lower than that of the OFDM counterpart [112], while the PAPR distributions of both schemes remain almost the same [7]. Note that as mentioned in [113], the distribution, rather than the maximum value, is considered to be a practical metric for evaluating the effects of the PAPR. In order to combat this detrimental effect of OFDM-IM, an alternative choice may be its time-domain counterpart, i.e., SCIM [15], which is shown in Fig. 2(b) and will be formally introduced later in Section V.
2) **Beneficial Low-Rate Region:** Additionally, the rate, in which OFDM-IM has an explicit advantage over OFDM, tends to be low. In [7], it has been demonstrated that the minimum Euclidean distance (MED) of OFDM-IM is clearly higher than that of OFDM only for $R_{\text{OFDM-IM}} \leq 3$ bps/Hz, while this gain diminishes quickly upon increasing the rate in the range of $R_{\text{OFDM-IM}} \geq 4$ bps/Hz. Note that the MED is a metric that corresponds to the achievable performance bound for an uncoded scenario under the assumption of an AWGN channel. Similarly, the performances of OFDM-IM and OFDM were compared in terms of the average mutual information (AMI) in [7] under the assumption of an independent and identically distributed (IID) frequency-flat Rayleigh fading channel. In that study, it was found that OFDM-IM exhibits an explicit performance gain over OFDM in the range of $R_{\text{OFDM-IM}} \leq 2$ bps/Hz. Let us also note that the AMI is a metric that provides an upper performance bound for scenarios employing capacity-achieving powerful channel coding schemes, such as turbo [31], [114] and low-density parity-check (LDPC) codes [115], [116].

## V. SINGLE-CARRIER INDEX MODULATION: IM IN THE TIME DIMENSION

The time-domain IM concept was originally developed as pulse position modulation (PPM) in the context of optical laser communications [70], [117] and ultra wideband (UWB) systems [118], [119] in order to achieve a high energy efficiency. Note that the time domain in the space-time IM of Section III-A is exploited in order to achieve a diversity gain, while the time-domain IM of this section is aimed at enhancing the achievable performance in a low-rate region, similar to OFDM-IM.

### A. TIME-DOMAIN SINGLE-CARRIER IM

Most recently, motivated by the development of OFDM-IM, its time-domain counterpart was proposed as SCIM in [15].[5] In SCIM, activating a subset of the serial time-domain symbols conveys additional information bits, besides those of the APSK-modulated symbols. In a similar manner to the relationship between OFDM and SC/FDMA-FDE [35], the OFDM-IM and SCIM/FDMA-FDE are close relatives. Fig. 2(b) shows the transceiver structure of SCIM. The frame-wise received signals $\mathbf{y}_t \in \mathbb{C}^{N_t}$ are represented by

$$\mathbf{y}_t = \mathbf{H}_t \mathbf{s}_t + \mathbf{n}, \tag{8}$$

where the $N_t$-length symbol vector $\mathbf{s}_t \in \mathbb{C}^{N_t}$ in each frame is divided into $P_t$ subframes of $\mathbf{s}_t = [\mathbf{s}_t^{(1)T} \cdots \mathbf{s}_t^{(P_t)T}]^T$, each subframe $\mathbf{s}_t^{(p)}$ having a length of $M_t = N_t/P_t$ symbols. In each subframe, $K_t$ out of the $M_t$ symbols are activated

[5] It is typically assumed that SCIM [15] operates in an uplink scenario with the aid of FDMA, similar to SC/FDMA [35], [36].

for sending $\mathcal{M}$-point APSK-modulated symbols. The other $M_t - K_t$ symbols are deactivated, i.e., set to zero symbols. After interleaving the $N_t$-length SCIM symbols by $\Pi$ and inserting a sufficiently long CP in advance of the interleaved block, the time-domain serial symbols are transmitted over the dispersive channel. The explicit advantage of the SCIM transmitter over its OFDM-IM counterpart is a low PAPR, which is the explicit benefit of SC transmissions. Note that interleaving $\Pi$ plays an important role in SCIM, since channel correlation between symbols in each subframe deteriorates the achievable detection performance. Hence, $N_t$ symbols in a frame $\mathbf{s}_t$ are interleaved in the time domain such that the symbols associated with each subframe $\mathbf{s}_t^{(p)}$ are separated as much as possible in the frame [15].

At the receiver, the CP is removed from the received signals, which are then interleaved by $\Pi^{-1}$, in order to arrive at the expression of (8). When the CP length is longer than the channel's tap length $\nu$, the channel matrix $\mathbf{H}_t$ has a circulant structure. This allows us to perform efficient $N_t$-point DFT-based eigenvalue decomposition of $\mathbf{H}_t$, hence enabling low-complexity diagonal minimum mean-square error (MMSE) equalization in the frequency domain, similar to SC/FDMA-FDE [35]. After FDE, SCIM symbols are detected by, for example, exhaustive search [15], compressed sensing [120], or log-likelihood detection [110]. Clearly, the detection complexity of SCIM is as low as that of OFDM-IM.

The normalized transmission rate of SCIM is represented by

$$R_{\mathrm{SCIM}} = \frac{K_t \log_2 \mathcal{M} + \left\lfloor \log_2 \binom{M_t}{K_t} \right\rfloor}{M_t} \quad [\mathrm{bps/Hz}]. \tag{9}$$

Comparisons of the SC and SCIM symbols are presented in Figs. 3(a) and 3(b), where in the comparison, the subframe length $M_t = 4$ and SCIM parameters $(K_t, M_t) = (1, 4)$ are considered. Hence, in SCIM, $K_t = 1$ out of the $M_t = 4$ symbols is activated, while an APSK-modulated symbol is transmitted from the single activated symbol. This implies that the number of information bits conveyed by the symbol activation is $\left\lfloor \log_2 \binom{4}{1} \right\rfloor = 2$, which corresponds to the second term of (9).

One explicit benefit of SCIM is a performance gain over the SC counterpart, especially in the low-rate region, which is similar to the relationship between OFDM-IM and OFDM. Moreover, in order to increase the already better transmission rate of SCIM, dual-mode SCIM was proposed in [17]. In dual-mode SCIM, a combination of two modulation modes conveys IM bits, while all the time-domain symbols are modulated, i.e., no zeros are inserted among the time-domain symbols.

In order to demonstrate the explicit benefit of SCIM, in Fig. 4 we compared the complementary cumulative distribution functions (CCDFs) of the PAPRs for the SC, SCIM, OFDM, and OFDM-IM schemes, where we considered the

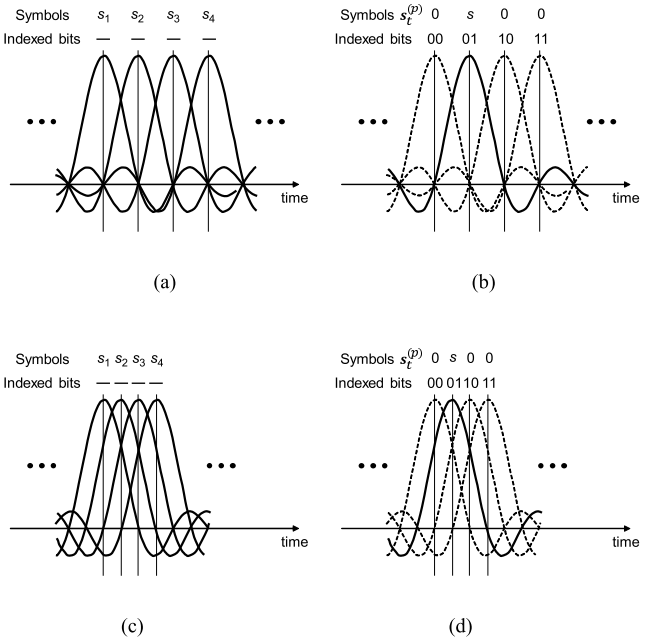


**FIGURE 3.** Time-domain signaling: (a) SC, (b) SCIM, (c) FTN, and (d) FTN-IM.

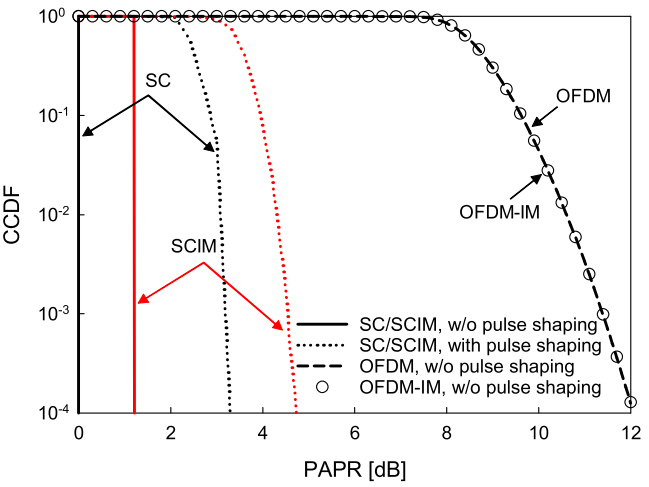


**FIGURE 4.** CCDFs of PAPRs in the SC, SCIM, OFDM, and OFDM-IM schemes, where the normalized transmission rate of 2 bps/Hz was considered.

normalized transmission rate of 2 bps/Hz. We assumed that $N_f = 1024$ subcarriers were used for OFDM and OFDM-IM, and that both the scenarios with and without pulse shaping were considered for SC and SCIM, according to [35]. Here, an RRC filter, having the roll-off factor of $\beta = 0.5$, was employed. Furthermore, the parameters of $(M_t, K_t) = (M_f, K_f) = (4, 3)$ were employed for OFDM-IM and SCIM, while the QPSK modulation was used for all the four schemes. Observe in Fig. 4 that the PAPR of SCIM was approximately 1.2 dB higher than that of SC, due to the sparse signaling in the time domain. However, both the SC and SCIM schemes exhibited a significantly lower PAPR than OFDM and OFDM-IM, as expected. Note that as

mentioned in [7], the CCDF of OFDM-IM was shown to be as high as that of OFDM.

### B. FASTER-THAN-NYQUIST SIGNALING WITH IM

FTN signaling was proposed in the 1970s [121], [122] as a means of breaking the ISI-free symbol interval limit, $T_0 = 1/(2W)$, which is determined by the Nyquist criterion, for the case that the symbols are strictly bandlimited to $W$ [Hz]. In FTN signaling, the symbol interval is simply shortened to $T = \alpha T_0$, where $\alpha < 1$ is the packing ratio, and an increase of a transmission rate is achieved without consuming any additional bandwidth [123]. The FTN signaling is shown in Fig. 3(c) as a contrast to the Nyquist-criterion-based signaling of Fig. 3(a). It was demonstrated that the rate of FTN signaling is boosted by a factor of $1/\alpha = 1.24$ for an uncoded scenario [122] and by a factor of $1/\alpha = 2$ for a channel-encoded scenario [123], which is achieved without any substantial performance loss relative to the Nyquist-criterion counterpart.

The main limitation of FTN signaling is severe ISI effects, which occur at the receiver. This naturally increases the detection complexity, for the sake of eliminating the ISI effects. To this end, diverse reduced-complexity equalizers have been proposed for the FTN receiver in the time domain [124], [125] and in the frequency domain [126]–[128]. However, although the decoding complexity is reduced with the aid of these efficient algorithms [124]–[128], the achievable performance of FTN is limited by the amount of FTN-specific ISI, as shown in the results of MED investigations [16], [122].

In order to improve the achievable performance bound of FTN, in [16] the concept of SCIM [15] was incorporated into FTN signaling, resulting in what is referred to as FTN-IM. In the FTN-IM scheme, a subset of FTN-symbol indices are activated while the other deactivated symbols are set to zeros, similar to in SCIM. As an explicit benefit of this sparse FTN-IM signaling, the FTN-specific ISI effects are reduced without substantially reducing the transmission rate. Hence, FTN-IM is capable of achieving a better BER performance than conventional FTN signaling while maintaining the rate boost. The signaling of FTN and FTN-IM is depicted in Figs. 3(c) and 3(d), respectively. FTN and FTN-IM have a similar relationship to that between SC and SCIM.

At the FTN-IM receiver, the received signals are firstly matched-filtered by an RRC shaping filter of $a^*(-t)$ and then the signals associated with the CP are removed in order to obtain the block-wise signals of [127]

$$\mathbf{y}_t = \mathbf{H}_t \mathbf{G}_t \mathbf{s}_t + \boldsymbol{\eta}, \tag{10}$$

where $\mathbf{G}_t \in \mathbb{R}^{N_t \times N_t}$ represents a circulant matrix, having the tap coefficient vector $\mathbf{g}_t = [g(-\xi T), \cdots, g(0), \cdots, g(\xi T)]^T$, which corresponds to the ISI effects induced by FTN signaling [127]. Here, $\xi$ is the effective tap length of FTN-induced ISI, while we have $g(t) = \int a(\tau) a^*(\tau - t) d\tau$. Furthermore, $\boldsymbol{\eta} \in \mathbb{C}^{N_t}$ represents colored (correlated) noises, which have the relationship $\mathbb{E}[\boldsymbol{\eta}(iT)\boldsymbol{\eta}^*(jT)] = N_0 g((i-j)T)$. In order to maintain circulant structures for $\mathbf{H_t}$ and $\mathbf{G_t}$, it is assumed that the CP length is set larger than the resultant tap length, which is caused by the FTN-induced ISI effects, as well as the long channel impulse response (CIR) dispersive channel. Note that symbol mapping of FTN-IM $\mathbf{s}_t$ in (10) is the same as that of SCIM in (8).

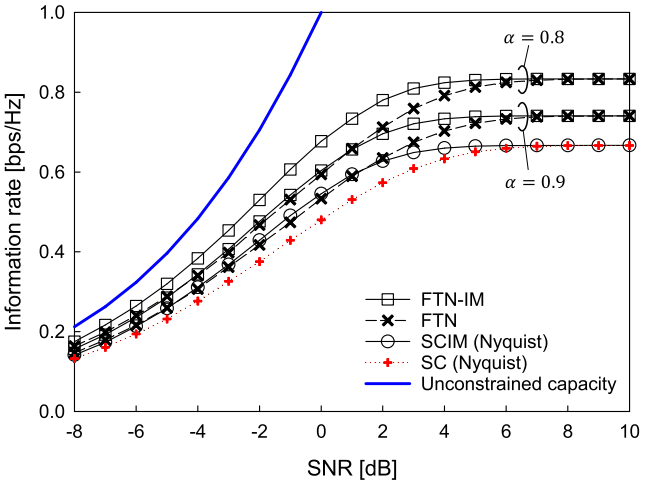


**FIGURE 5.** Information rates of the SC, SCIM, FTN, and FTN-IM schemes under the assumptions of an AWGN channel. The RRC filter, having the roll-off factor of $\beta = 0.5$, was employed for all the schemes.

The received signal model of FTN-IM in (10) is similar to that of SCIM in (9), except that the effects of FTN-specific ISI are seen as $\mathbf{G}_t$ in (10). Hence, at the receiver, low-complexity FDE can be carried out, according to [16].

Fig. 5 compares the constrained information rates [30] of the SC, SCIM, FTN, and FTN-IM schemes assuming an AWGN channel. In the comparisons, the roll-off factor of the RRC filter was maintained to be $\beta = 0.5$ for all the schemes, and the packing ratio was varied from $\alpha = 0.8$ to 0.9 for the FTN and the FTN-IM schemes. Also, BPSK modulation was employed for the SC and the FTN schemes, while IM parameters $(M_t, K_t) = (4, 1)$ were employed for SCIM and FTN-IM with the aid of QPSK modulation. Observe in Fig. 5 that the FTN-IM scheme outperformed the other three SC schemes. More specifically, the limited performance gain of SCIM over its SC counterpart was seen in the SNR range between $-5$ dB and 5 dB, as expected from that of OFDM-IM over OFDM [7]. The incorporation of the FTN concept into SCIM enables us to achieve a higher performance gain, as illustrated by the FTN-IM curves of Fig. 5.

## VI. FUTURE CHALLENGES

Several fundamental limitations imposed on the IM schemes were highlighted in the previous sections. In this section, we provide a more detailed discussion, as well as describe potential future directions.

### A. TIME-LIMITED PULSE-SHAPING CONSTRAINT IN SPATIAL MODULATION

A single-RF spatial modulation transmitter has to send a time-limited pulse, due to the antenna-switching mechanism

shown in Fig. 1(a). Hence, a bandwidth-efficient time-orthogonal shaping filter is unavailable, and so a bandwidth-inefficient time-limited shaping filter has to be employed. Therefore, the bandwidth efficiency of single-RF spatial modulation suffers a penalty, in comparison to those of the other full-RF systems shown in Fig. 1(b), which support the use of a bandwidth-efficient time-orthogonal shaping filter. Note that the single-RF IM schemes in the spatial domain, which are listed in Table 2, such as the spatial modulation, rectangular DSM, quadrature spatial modulation, ASTSK, ADSTSK, DSM, and beamspace IM schemes, have this limitation, and the same holds true for GSM, since it also relies on antenna activation with the reduced number of RF chains.

However, in most of the previous studies, the performance advantages of single-RF spatial modulation over conventional full-RF modems were typically discussed without taking into account this limitation. Exceptions are [129] and [60]: the need of time-limited pulse shaping for single-RF spatial modulation was mentioned in [129], while fair performance comparisons with the conventional full-RF MIMO employing time-orthogonal pulse shaping were provided in [60]. More detailed performance comparisons between single-RF spatial modulation and other classic full-RF MIMO schemes, such as both link- and system-level investigations, remain left for future studies. Moreover, investigating the effects of time-limited pulse shaping on the energy efficiency of a power amplifier is also an open issue.

One approach for reducing this bandwidth-expansion effect is to increase the number of RF chains at the spatial modulation transmitter. For example, the employment of two RF chains allows an overlap of two time-domain symbols, which improves the bandwidth efficiency, as presented in [60]. Naturally, this benefit is achieved at the cost of increasing the static power consumption and of increasing the transmitter cost.

In addition to the aforementioned bandwidth-expansion effect, the impact of switching time in single-RF spatial modulation was evaluated in [130], which found that switching time on the order of nanoseconds deteriorates the transmission rate, due to the introduction of systematic pauses. This deterioration may become especially severe in the case of a very high transmission rate, i.e., very frequent antenna switching, because SC transmissions are required for the single-RF spatial modulation.

### B. SINGLE-CARRIER LIMITATION IN SPATIAL MODULATION

As mentioned in [46], single-RF spatial modulation is not capable of achieving any significant performance gain over the single-antenna and conventional full-RF MIMO schemes when used with OFDM. More specifically, subcarrier-based antenna activation in OFDM would require simultaneous activation of multiple different transmit antenna elements, hence requiring full-RF chains. By contrast, although frame-based antenna activation allows single-RF operation in

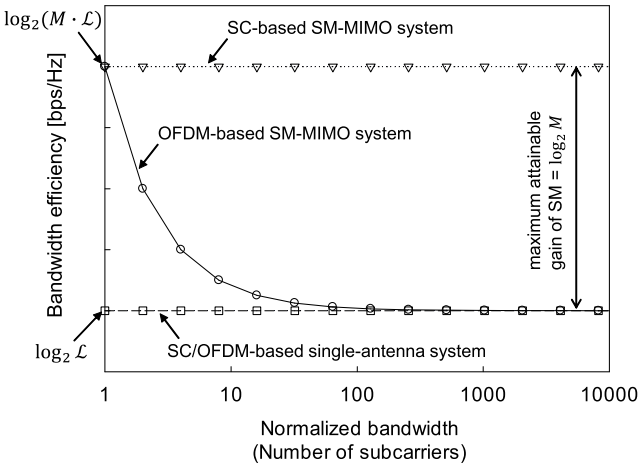


**FIGURE 6. Bandwidth efficiencies of the broadband OFDM-based and SC-based SM-MIMO systems; that of the classic SC/OFDM-based single antenna system is included as a benchmark. The parameters $(M, \mathcal{L})$ of Fig. 6 are considered to be $(N_{\rm tx}, \mathcal{M})$ in this paper. (©IEEE. Reprinted, with permission, from [46] Sugiura and Hanzo.)**

OFDM, the performance gain attained from antenna activation becomes marginal. This is because the number of subcarriers used for OFDM is typically on the order of thousands. Hence, in order to achieve an energy- and cost-efficient single-RF spatial modulation transmitter structure in a broadband wireless scenario, it is necessary to employ SC transmissions rather than multicarrier ones. Performance comparisons between single-RF OFDM and SC spatial modulation schemes are provided in Fig. 6 [46], where the achievable performance gain of the OFDM-based spatial modulation over the single-antenna-based system is shown to diminish upon increasing the number of subcarriers, while that of the SC-based spatial modulation remains unchanged across the entire bandwidth region. It is thus clarified that single-RF spatial modulation requires SC transmissions.

In accordance with the SC limitation, the broadband single-RF SC spatial modulation system typically experiences a frequency-selective channel having a long tap. The associated spatial modulation receiver has to rely on equalization. This implies that the detection algorithms of spatial modulation, which were developed for a frequency-flat channel, are directly applicable only in an unrealistic narrowband scenario. By contrast, a number of low-complexity spatial modulation equalization techniques have been developed in [46], [51], and [131]–[133].

### C. ABSENCE OF ANTENNA SCALABILITY IN DSM

The main limitation of DSM is its unscalability with respect to the number of transmit antenna elements. More specifically, DSM relies on the transmission of a differentially encoded (square) unitary matrix, and hence the number of symbol intervals per block is the same as the number of transmit antenna elements $N_{\rm tx}$. This indicates that upon increasing the number of transmit antenna elements while maintaining the code rate, the number of legitimate unitary matrices

**TABLE 3. List of acronyms.**

| | |
|---|---|
| AF | Amplify-and-Forward |
| APSK | Amplitude and Phase Shift Keying |
| ASTSK | Asynchronous Space-Time Shift Keying |
| ADSTSK | Asynchronous Differential Space-Time Shift Keying |
| AWGN | Additive White Gaussian Noise |
| BER | Bit Error Rate |
| CCDF | Complementary Cumulative Distribution Function |
| CDMA | Code Division Multiple Access |
| CP | Cyclic Prefix |
| CSIR | Channel State Information at the Receiver |
| CSIT | Channel State Information at the Transmitter |
| D/A | Digital-to-Analog |
| DF | Decode-and-Forward |
| DFT | Discrete Fourier Transform |
| DSM | Differential Spatial Modulation |
| DSTSK | Differential Space-Time Shift Keying |
| FDE | Frequency-Domain Equalization |
| FDMA | Frequency Division Multiple Access |
| FHSS | Frequency-Hopping Spread Spectrum |
| FTN | Faster-Than-Nyquist |
| FTN-IM | Faster-Than-Nyquist with Index Modulation |
| GSM | Generalized Spatial Modulation |
| GSTSK | Generalized Space-Time Shift Keying |
| IID | Independent and Identically Distributed |
| ISI | Inter-Symbol Interference |
| LDPC | Low-Density Parity-Check |
| LLR | Log-Likelihood Ratio |
| MED | Minimum Euclidean Distance |
| MIMO | Multiple-Input Multiple-Output |
| ML | Maximum-Likelihood |
| MMSE | Minimum Mean-Squared Error |
| NOMA | Non-Orthogonal Multiple Access |
| IM | Index Modulation |
| ISI | Inter-Symbol Interference |
| OFDM | Orthogonal Frequency-Division Multiplexing |
| OSTBC | Orthogonal Space-Time Block Coding |
| PAPR | Peak-to-Average Power Ratio |
| PDF | Probability Density Function |
| PSK | Phase Shift Keying |
| PPM | Pulse Position Modulation |
| QAM | Quadrature Amplitude Modulation |
| RDSM | Rectangular Differential Spatial Modulation |
| RF | Radio Frequency |
| RRC | Root Raised Cosine |
| S/P | Signal-to-Parallel |
| SC | Single-Carrier |
| SCIM | Single-Carrier Index Modulation |
| SIM | Subcarrier Index Modulation |
| SS | Spectrum Spreading |
| SSK | Space-Shift keying |
| STFSK | Space-Time-Frequency Shift Keying |
| STSK | Space-Time Shift Keying |
| TD | Time-Domain |
| TDD | Time-Division Duplex |
| TDE | Time-Domain Equalization |
| UDSTC | Unitary Differential Space-Time Modulation |
| UWB | Ultra WideBand |

increases exponentially. Therefore, it is a challenging task to achieve a high transmission rate when considering a high number of transmit antenna elements in DSM.

The above is the main reason why almost all of the previous DSM studies [19], [24], [101], [102], [104]–[109] only considered $N_{\rm tx} \leq 3$, or at most $N_{\rm tx} = 4$ with a low transmission rate, transmit antenna elements.[6]

### D. NARROWBAND LIMITATION OF DSM

The SC limitation of Section VI-B imposed on single-RF spatial modulation is more challenging in the case of single-RF DSM arrangements [101], [102], [104]–[107], [109], [134]. Since single-RF DSM may not be used with multicarrier transmissions, similar to the case of its coherent spatial modulation counterpart, it has to rely on SC transmission. Broadband SC transmissions experience a severe delay spread, hence requiring equalization at the receiver. However, in general, non-coherent channel equalization is an open issue, and hence single-RF DSM operates only in a frequency-flat (narrowband) channel. Developing a practical SC DSM scheme, i.e., operating in a broadband scenario, is left for future studies.

### E. LOW-RATE BENEFITS OF OFDM-IM AND SCIM

As mentioned above, the explicit performance advantages of OFDM-IM and SCIM/FDMA over their full-symbol-allocation counterparts, i.e., OFDM and SC/FDMA, are limited to a low-rate region. Hence, the scenarios to which OFDM-IM and SCIM/FDMA are applied have to be carefully considered. For example, operation in a low-rate multiple access scenario supporting many connections requiring high reliability and low latency may benefit from OFDM-IM and SCIM/FDMA.[7] The development of techniques for improving the rate in the cases of OFDM-IM and SCIM/FDMA is also an open issue.

## VII. CONCLUSIONS

In this paper, we have reviewed the state-of-the-art designs of several IM arrangements that exploit the space, time, and frequency domains. Furthermore, we clarified several IM-specific merits relative to the conventional bandwidth-efficient counterparts, i.e., spatial multiplexing, OFDM, and SC/FDMA. More specifically, we characterized the operational scenarios and the system settings which are specifically beneficial for the IM schemes versus their non-IM counterparts, while clarifying the fundamental limitations and the open issues, which have not been sufficiently explored previously. Finally, we presented the rationale of the recent novel IM scheme that amalgamates the time-domain IM scheme and FTN signaling.

## REFERENCES

[1] M. Di Renzo, H. Haas, and P. M. Grant, "Spatial modulation for multiple-antenna wireless systems: A survey," *IEEE Commun. Mag.*, vol. 49, no. 12, pp. 182–191, Dec. 2011.

[6] Although an exception is found in [134], where $N_{\rm tx} > 4$ is considered, the transmission rate is quite low, due to the limitation imposed by the use of square unitary matrices.

[7] By contrast, spatial modulation has the exclusive benefit of having a single-RF transmitter structure, as opposed to spatial multiplexing.

[2] S. Sugiura, S. Chen, and L. Hanzo, "A universal space-time architecture for multiple-antenna aided systems," *IEEE Commun. Surveys Tuts.*, vol. 14, no. 2, pp. 401–420, 2nd Quart., 2012.

[3] M. Di Renzo, H. Haas, A. Ghrayeb, S. Sugiura, and L. Hanzo, "Spatial modulation for generalized MIMO: Challenges, opportunities, and implementation," *Proc. IEEE*, vol. 102, no. 1, pp. 56–103, Jan. 2014.

[4] M. I. Kadir, S. Sugiura, S. Chen, and L. Hanzo, "Unified MIMO-multicarrier designs: A space–time shift keying approach," *IEEE Commun. Surveys Tuts.*, vol. 17, no. 2, pp. 550–579, 2nd Quart., 2015.

[5] P. Yang, M. Di Renzo, Y. Xiao, S. Li, and L. Hanzo, "Design guidelines for spatial modulation," *IEEE Commun. Surveys Tuts.*, vol. 17, no. 1, pp. 6–26, 1st Quart., 2015.

[6] P. Yang *et al.*, "Single-carrier SM-MIMO: A promising design for broadband large-scale antenna systems," *IEEE Commun. Surveys Tuts.*, vol. 18, no. 3, pp. 1687–1716, 3rd Quart., 2016.

[7] N. Ishikawa, S. Sugiura, and L. Hanzo, "Subcarrier-index modulation aided OFDM—Will it work?" *IEEE Access*, vol. 4, pp. 2580–2593, 2016.

[8] E. Başar, "Index modulation techniques for 5G wireless networks," *IEEE Commun. Mag.*, vol. 54, no. 7, pp. 168–175, Jul. 2016.

[9] M. Di Renzo, H. Haas, A. Ghrayeb, L. Hanzo, and S. Sugiura, "Spatial modulation for multiple-antenna communication," in *Wiley Encyclopedia of Electrical and Electronics Engineering*. New York, NY, USA: Wiley, Nov. 2016.

[10] E. Başar, M. Wen, R. Mesleh, M. Di Renzo, Y. Xiao, and H. Haas, "Index modulation techniques for next-generation wireless networks," *IEEE Access*, vol. 5, pp. 16693–16746, 2017.

[11] L. Hanzo, S. X. Ng, W. Webb, and T. Keller, *Quadrature Amplitude Modulation: From Basics to Adaptive Trellis-Coded, Turbo-Equalised and Space-Time Coded OFDM, CDMA and MC-CDMA Systems*. Hoboken, NJ, USA: Wiley, 2004.

[12] R. Y. Mesleh, H. Haas, S. Sinanovic, C. W. Ahn, and S. Yun, "Spatial modulation," *IEEE Trans. Veh. Technol.*, vol. 57, no. 4, pp. 2228–2241, Jul. 2008.

[13] J. Jeganathan, A. Ghrayeb, and L. Szczecinski, "Spatial modulation: Optimal detection and performance analysis," *IEEE Commun. Lett.*, vol. 12, no. 8, pp. 545–547, Aug. 2008.

[14] J. Jeganathan, A. Ghrayeb, L. Szczecinski, and A. Ceron, "Space shift keying modulation for MIMO channels," *IEEE Trans. Wireless Commun.*, vol. 8, no. 7, pp. 3692–3703, Jul. 2009.

[15] M. Nakao, T. Ishihara, and S. Sugiura, "Single-carrier frequency-domain equalization with index modulation," *IEEE Commun. Lett.*, vol. 21, no. 2, pp. 298–301, Feb. 2017.

[16] T. Ishihara and S. Sugiura, "Faster-than-Nyquist signaling with index modulation," *IEEE Wireless Commun. Lett.*, vol. 6, no. 5, pp. 630–633, Oct. 2017.

[17] M. Nakao and S. Sugiura, "Dual-mode time-domain single-carrier index modulation with frequency-domain equalization," in *Proc. IEEE 86th Veh. Technol. Conf.*, Toronto, ON, Canada, Sep. 2017, pp. 1–5.

[18] P. K. Frenger and N. A. B. Svensson, "Parallel combinatory OFDM signaling," *IEEE Trans. Commun.*, vol. 47, no. 4, pp. 558–567, Apr. 1999.

[19] S. Sugiura, S. Chen, and L. Hanzo, "Coherent and differential space-time shift keying: A dispersion matrix approach," *IEEE Trans. Commun.*, vol. 58, no. 11, pp. 3219–3230, Nov. 2010.

[20] S. Sugiura, S. Chen, and L. Hanzo, "Generalized space-time shift keying designed for flexible diversity-, multiplexing- and complexity-tradeoffs," *IEEE Trans. Wireless Commun.*, vol. 10, no. 4, pp. 1144–1153, Apr. 2011.

[21] H. A. Ngo, C. Xu, S. Sugiura, and L. Hanzo, "Space-time-frequency shift keying for dispersive channels," *IEEE Signal Process. Lett.*, vol. 18, no. 3, pp. 177–180, Mar. 2011.

[22] M. I. Kadir, S. Sugiura, J. Zhang, S. Chen, and L. Hanzo, "OFDMA/SC-FDMA aided space–time shift keying for dispersive multiuser scenarios," *IEEE Trans. Veh. Technol.*, vol. 62, no. 1, pp. 408–414, Jan. 2013.

[23] A. Kalis, A. G. Kanatas, and C. B. Papadias, "A novel approach to MIMO transmission using a single RF front end," *IEEE J. Sel. Areas Commun.*, vol. 26, no. 6, pp. 972–980, Aug. 2008.

[24] S. Sugiura, "Coherent versus non-coherent reconfigurable antenna aided virtual MIMO systems," *IEEE Signal Process. Lett.*, vol. 21, no. 4, pp. 390–394, Apr. 2014.

[25] S. Sugiura, S. Chen, H. Haas, P. M. Grant, and L. Hanzo, "Coherent versus non-coherent decode-and-forward relaying aided cooperative space-time shift keying," *IEEE Trans. Commun.*, vol. 59, no. 6, pp. 1707–1719, Jun. 2011.

[26] R. Mesleh, S. Ikki, and M. Alwakeel, "Performance analysis of space shift keying with amplify and forward relaying," *IEEE Commun. Lett.*, vol. 15, no. 12, pp. 1350–1352, Dec. 2011.

[27] Y. Yang and S. Aissa, "Information-guided transmission in decode-and-forward relaying systems: Spatial exploitation and throughput enhancement," *IEEE Trans. Wireless Commun.*, vol. 10, no. 7, pp. 2341–2351, Jul. 2011.

[28] S. Narayanan, M. Di Renzo, F. Graziosi, and H. Haas, "Distributed spatial modulation: A cooperative diversity protocol for half-duplex relay-aided wireless networks," *IEEE Trans. Veh. Technol.*, vol. 65, no. 5, pp. 2947–2964, May 2016.

[29] A. J. Paulraj, D. A. Gore, R. U. Nabar, and H. Bolcskei, "An overview of MIMO communications—A key to gigabit wireless," *Proc. IEEE*, vol. 92, no. 2, pp. 198–218, Feb. 2004.

[30] L. Hanzo, O. Alamri, M. El-Hajjar, and N. Wu, *Near-Capacity Multi-Functional MIMO Systems: Sphere-Packing, Iterative Detection and Cooperation*. Hoboken, NJ, USA: Wiley, 2009.

[31] S. Sugiura, S. Chen, and L. Hanzo, "MIMO-aided near-capacity turbo transceivers: Taxonomy and performance versus complexity," *IEEE Commun. Surveys Tuts.*, vol. 14, no. 2, pp. 421–442, 2nd Quart., 2012.

[32] C. Xu, S. Sugiura, S. X. Ng, P. Zhang, L. Wang, and L. Hanzo, "Two decades of MIMO design tradeoffs and reduced-complexity MIMO detection in near-capacity systems," *IEEE Access*, vol. 5, pp. 18564–18632, 2017.

[33] R. Van Nee and R. Prasad, *OFDM for Wireless Multimedia Communications*. Norwood, MA, USA: Artech House, 2000.

[34] L. Hanzo, M. Münster, B. Choi, and T. Keller, *OFDM and MC-CDMA for Broadband Multi-User Communications, WLANs and Broadcasting*. Hoboken, NJ, USA: Wiley, 2003.

[35] H. G. Myung, J. Lim, and D. J. Goodman, "Single carrier FDMA for uplink wireless transmission," *IEEE Veh. Technol. Mag.*, vol. 1, no. 3, pp. 30–38, Sep. 2006.

[36] F. Pancaldi, G. M. Vitetta, R. Kalbasi, N. Al-Dhahir, M. Uysal, and H. Mheidat, "Single-carrier frequency domain equalization," *IEEE Signal Process. Mag.*, vol. 25, no. 5, pp. 37–56, Sep. 2008.

[37] S. Sesia, M. Baker, and I. Toufik, *LTE—The UMTS Long Term Evolution: From Theory to Practice*. Hoboken, NJ, USA: Wiley, 2011.

[38] J. G. Andrews, A. Ghosh, and R. Muhamed, *Fundamentals of WiMAX: Understanding Broadband Wireless Networking*. London, U.K.: Pearson Education, 2007.

[39] J. G. Andrews *et al.*, "What will 5G be?" *IEEE J. Sel. Areas Commun.*, vol. 32, no. 6, pp. 1065–1082, Jun. 2014.

[40] A. Gupta and R. K. Jha, "A survey of 5G network: Architecture and emerging technologies," *IEEE Access*, vol. 3, pp. 1206–1232, 2015.

[41] Y. A. Chau and S.-H. Yu, "Space modulation on wireless fading channels," in *Proc. IEEE 54th Veh. Technol. Conf.*, vol. 3. Atlantic City, NJ, USA, Oct. 2001, pp. 1668–1671.

[42] H. Haas, E. Costa, and E. Schulz, "Increasing spectral efficiency by data multiplexing using antenna arrays," in *Proc. IEEE Int. Symp. Pers., Indoor Mobile Radio Commun.*, vol. 2. Lisbon, Portugal, Sep. 2002, pp. 610–613.

[43] S. Sugiura and L. Hanzo, "On the joint optimization of dispersion matrices and constellations for near-capacity irregular precoded space-time shift keying," *IEEE Trans. Wireless Commun.*, vol. 12, no. 1, pp. 380–387, Jan. 2013.

[44] P. Yang, Y. Xiao, L. Yin, Q. Tang, S. Li, and L. Hanzo, "Hybrid bit-to-symbol mapping for spatial modulation," *IEEE Trans. Veh. Technol.*, vol. 65, no. 7, pp. 5804–5810, Jul. 2016.

[45] S. Althunibat and R. Mesleh, "A bit-to-symbol mapping scheme for spatial modulation with partial channel state information," *IEEE Commun. Lett.*, vol. 21, no. 5, pp. 995–998, May 2017.

[46] S. Sugiura and L. Hanzo, "Single-RF spatial modulation requires single-carrier transmission: Frequency-domain turbo equalization for dispersive channels," *IEEE Trans. Veh. Technol.*, vol. 64, no. 10, pp. 4870–4875, Oct. 2015.

[47] S. Sugiura, C. Xu, S. X. Ng, and L. Hanzo, "Reduced-complexity coherent versus non-coherent QAM-aided space-time shift keying," *IEEE Trans. Commun.*, vol. 59, no. 11, pp. 3090–3101, Nov. 2011.

[48] A. Younis, S. Sinanovic, M. Di Renzo, R. Mesleh, and H. Haas, "Generalised sphere decoding for spatial modulation," *IEEE Trans. Commun.*, vol. 61, no. 7, pp. 2805–2815, Jul. 2013.

[49] C. Xu, S. Sugiura, S. X. Ng, and L. Hanzo, "Spatial modulation and space-time shift keying: Optimal performance at a reduced detection complexity," *IEEE Trans. Commun.*, vol. 61, no. 1, pp. 206–216, Jan. 2013.

[50] R. Rajashekar, K. V. S. Hari, and L. Hanzo, "Reduced-complexity ML detection and capacity-optimized training for spatial modulation systems," *IEEE Trans. Commun.*, vol. 62, no. 1, pp. 112–125, Jan. 2014.
[51] R. Rajashekar, K. V. S. Hari, and L. Hanzo, "Spatial modulation aided zero-padded single carrier transmission for dispersive channels," *IEEE Trans. Commun.*, vol. 61, no. 6, pp. 2318–2329, Jun. 2013.
[52] A. Stavridis, S. Sinanovic, M. Di Renzo, and H. Haas, "Energy evaluation of spatial modulation at a multi-antenna base station," in *Proc. IEEE 78th Veh. Technol. Conf.*, Las Vegas, NV, USA, Sep. 2013, pp. 1–5.
[53] C.-L. I., C. Rowell, S. Han, Z. Xu, G. Li, and Z. Pan, "Toward green and soft: A 5G perspective," *IEEE Commun. Mag.*, vol. 52, no. 2, pp. 66–73, Feb. 2014.
[54] P. Yang, Y. Xiao, Y. Yu, and S. Li, "Adaptive spatial modulation for wireless MIMO transmission systems," *IEEE Commun. Lett.*, vol. 15, no. 6, pp. 602–604, Jun. 2011.
[55] P. Yang, Y. Xiao, L. Li, Q. Tang, Y. Yu, and S. Li, "Link adaptation for spatial modulation with limited feedback," *IEEE Trans. Veh. Technol.*, vol. 61, no. 8, pp. 3808–3813, Oct. 2012.
[56] R. Rajashekar, K. V. S. Hari, and L. Hanzo, "Antenna selection in spatial modulation systems," *IEEE Commun. Lett.*, vol. 17, no. 3, pp. 521–524, Mar. 2013.
[57] R. Zhang, L. Yang, and L. Hanzo, "Generalised pre-coding aided spatial modulation," *IEEE Trans. Wireless Commun.*, vol. 12, no. 11, pp. 5434–5443, Nov. 2013.
[58] N. Ishikawa and S. Sugiura, "Maximizing constrained capacity of power-imbalanced optical wireless MIMO communications using spatial modulation," *J. Lightw. Technol.*, vol. 33, no. 2, pp. 519–527, Jan. 15, 2015.
[59] T. Handte, A. Müller, and J. Speidel, "BER analysis and optimization of generalized spatial modulation in correlated fading channels," in *Proc. IEEE 70th Veh. Technol. Conf. Fall*, Anchorage, AK, USA, Sep. 2009, pp. 1–5.
[60] K. Ishibashi and S. Sugiura, "Effects of antenna switching on band-limited spatial modulation," *IEEE Wireless Commun. Lett.*, vol. 3, no. 4, pp. 345–348, Aug. 2014.
[61] J. Jeganathan, A. Ghrayeb, and L. Szczecinski, "Generalized space shift keying modulation for MIMO channels," in *Proc. IEEE 19th Int. Symp. Pers., Indoor Mobile Radio Commun.*, Cannes, France, Sep. 2008, pp. 1–5.
[62] S. Chen, S. Sugiura, and L. Hanzo, "Semi-blind joint channel estimation and data detection for space-time shift keying systems," *IEEE Signal Process. Lett.*, vol. 17, no. 12, pp. 993–996, Dec. 2010.
[63] N. Ishikawa and S. Sugiura, "Rectangular differential spatial modulation for open-loop noncoherent massive-MIMO downlink," *IEEE Trans. Wireless Commun.*, vol. 16, no. 3, pp. 1908–1920, Mar. 2017.
[64] R. Mesleh, S. S. Ikki, and H. M. Aggoune, "Quadrature spatial modulation," *IEEE Trans. Veh. Technol.*, vol. 64, no. 6, pp. 2738–2742, Jun. 2015.
[65] B. L. Hughes, "Differential space-time modulation," *IEEE Trans. Inf. Theory*, vol. 46, no. 7, pp. 2567–2578, Nov. 2000.
[66] B. M. Hochwald and W. Sweldens, "Differential unitary space-time modulation," *IEEE Trans. Commun.*, vol. 48, no. 12, pp. 2041–2052, Dec. 2000.
[67] S. Sasaki, J. Zhu, and G. Marubayashi, "Performance of parallel combinatory spread spectrum multiple access communication systems," in *Proc. IEEE Int. Symp. Pers., Indoor Mobile Radio Commun.*, Sep. 1991, pp. 204–208.
[68] F. Xu, C. Zhan, Y. Xie, and D. Wang, "Performance of CZT-assisted parallel combinatory multicarrier frequency-hopping spread spectrum over shallow underwater acoustic channels," *Ocean Eng.*, vol. 110, pp. 116–125, Dec. 2015.
[69] T. Mao, Z. Wang, Q. Wang, S. Chen, and L. Hanzo, "Dual-mode index modulation aided OFDM," *IEEE Access*, vol. 5, pp. 50–60, 2017.
[70] J. Pierce, "Optical channels: Practical limits with photon counting," *IEEE Trans. Commun.*, vol. COM-26, no. 12, pp. 1819–1821, Dec. 1978.
[71] J. Wang, S. Jia, and J. Song, "Generalised spatial modulation system with multiple active transmit antennas and low complexity detection scheme," *IEEE Trans. Wireless Commun.*, vol. 11, no. 4, pp. 1605–1615, Apr. 2012.
[72] P. S. Kildal and K. Rosengren, "Correlation and capacity of MIMO systems and mutual coupling, radiation efficiency, and diversity gain of their antennas: Simulations and measurements in a reverberation chamber," *IEEE Commun. Mag.*, vol. 42, no. 12, pp. 104–112, Dec. 2004.
[73] R. Schlub, J. Lu, and T. Ohira, "Seven-element ground skirt monopole ESPAR antenna design from a genetic algorithm and the finite element method," *IEEE Trans. Antennas Propag.*, vol. 51, no. 11, pp. 3033–3039, Nov. 2003.
[74] S. Sugiura and H. Iizuka, "Reactively steered ring antenna array for automotive application," *IEEE Trans. Antennas Propag.*, vol. 55, no. 7, pp. 1902–1908, Jul. 2007.
[75] S. Sugiura, N. Suzuki, and H. Iizuka, "Effect of number of elements of a reactively loaded ring antenna array on the performance of beamwidth variation," *IEEE Antennas Wireless Propag. Lett.*, vol. 7, pp. 669–672, 2008.
[76] S. Sugiura, "A review of recent patents on reactance-loaded reconfigurable antennas," *Recent Patents Elect. Electron. Eng.*, vol. 2, no. 3, pp. 200–206, 2009.
[77] Z. Bouida, H. El-Sallabi, A. Ghrayeb, and K. A. Qaraqe, "Reconfigurable antenna-based space-shift keying (SSK) for MIMO Rician channels," *IEEE Trans. Wireless Commun.*, vol. 15, no. 1, pp. 446–457, Jan. 2016.
[78] T. L. Marzetta, "Noncooperative cellular wireless with unlimited numbers of base station antennas," *IEEE Trans. Wireless Commun.*, vol. 9, no. 11, pp. 3590–3600, Nov. 2010.
[79] F. Rusek *et al.*, "Scaling up MIMO: Opportunities and challenges with very large arrays," *IEEE Signal Process. Mag.*, vol. 30, no. 1, pp. 40–60, Jan. 2013.
[80] E. G. Larsson, O. Edfors, F. Tufvesson, and T. L. Marzetta, "Massive MIMO for next generation wireless systems," *IEEE Commun. Mag.*, vol. 52, no. 2, pp. 186–195, Feb. 2014.
[81] N. Ishikawa, R. Rajashekar, S. Sugiura, and L. Hanzo, "Generalized-spatial-modulation-based reduced-RF-chain millimeter-wave communications," *IEEE Trans. Veh. Technol.*, vol. 66, no. 1, pp. 879–883, Jan. 2017.
[82] G. Wunder *et al.*, "5GNOW: Non-orthogonal, asynchronous waveforms for future mobile applications," *IEEE Commun. Mag.*, vol. 52, no. 2, pp. 97–105, Feb. 2014.
[83] Z. Ding, F. Adachi, and H. V. Poor, "The application of MIMO to non-orthogonal multiple access," *IEEE Trans. Wireless Commun.*, vol. 15, no. 1, pp. 537–552, Jan. 2016.
[84] X. Zhu, Z. Wang, and J. Cao, "NOMA-based spatial modulation," *IEEE Access*, vol. 5, pp. 3790–3800, 2017.
[85] Y. Chen, L. Wang, Y. Ai, B. Jiao, and L. Hanzo, "Performance analysis of NOMA-SM in vehicle-to-vehicle massive MIMO channels," *IEEE J. Sel. Areas Commun.*, to be published, doi: 10.1109/JSAC.2017.2726006.
[86] X. Wang, J. Wang, L. He, Z. Tang, and J. Song, "On the achievable spectral efficiency of spatial modulation aided downlink non-orthogonal multiple access," *IEEE Commun. Lett.*, vol. 21, no. 9, pp. 1937–1940, Sep. 2017.
[87] A. Afana, T. M. N. Ngatched, and O. A. Dobre, "Spatial modulation in MIMO limited-feedback spectrum-sharing systems with mutual interference and channel estimation errors," *IEEE Commun. Lett.*, vol. 19, no. 10, pp. 1754–1757, Oct. 2015.
[88] Z. Bouida, A. Ghrayeb, and K. A. Qaraqe, "Adaptive spatial modulation for spectrum sharing systems with limited feedback," *IEEE Trans. Commun.*, vol. 63, no. 6, pp. 2001–2014, Jun. 2015.
[89] A. Alizadeh, H. R. Bahrami, and M. Maleki, "Performance analysis of spatial modulation in overlay cognitive radio communications," *IEEE Trans. Commun.*, vol. 64, no. 8, pp. 3220–3232, Aug. 2016.
[90] E. Biglieri, A. J. Goldsmith, L. J. Greenstein, N. B. Mandayam, and H. V. Poor, *Principles of Cognitive Radio*. New York, NY, USA: Cambridge Univ. Press, 2012.
[91] S. Sugiura, "Dispersion matrix optimization for space-time shift keying," *IEEE Commun. Lett.*, vol. 15, no. 11, pp. 1152–1155, Nov. 2011.
[92] C. Xu, S. Sugiura, S. X. Ng, and L. Hanzo, "Reduced-complexity soft-decision aided space-time shift keying," *IEEE Signal Process. Lett.*, vol. 18, no. 10, pp. 547–550, Oct. 2011.
[93] S. Sugiura, C. Xu, S. X. Ng, and L. Hanzo, "Reduced-complexity iterative-detection-aided generalized space-time shift keying," *IEEE Trans. Veh. Technol.*, vol. 61, no. 8, pp. 3656–3664, Oct. 2012.
[94] E. Başar, Ü. Aygölü, E. Panayırcı, and H. V. Poor, "Space-time block coded spatial modulation," *IEEE Trans. Commun.*, vol. 59, no. 3, pp. 823–832, Mar. 2011.
[95] D. Yang, C. Xu, L. L. Yang, and L. Hanzo, "Transmit-diversity-assisted space-shift keying for colocated and distributed/cooperative MIMO elements," *IEEE Trans. Veh. Technol.*, vol. 60, no. 6, pp. 2864–2869, Jul. 2011.
[96] P. W. Wolniansky, G. J. Foschini, G. D. Golden, and R. A. Valenzuela, "V-BLAST: An architecture for realizing very high data rates over the rich-scattering wireless channel," in *Proc. Int. Symp. Signals, Syst., Electron.*, Pisa, Italy, 1998, pp. 295–300.

[97] S. M. Alamouti, "A simple transmit diversity technique for wireless communications," *IEEE J. Sel. Areas Commun.*, vol. SAC-16, no. 8, pp. 1451–1458, Oct. 1988.
[98] V. Tarokh, N. Seshadri, and A. R. Calderbank, "Space-time codes for high data rate wireless communication: Performance criterion and code construction," *IEEE Trans. Inf. Theory*, vol. 44, no. 2, pp. 744–765, Mar. 1998.
[99] M. Di Renzo and H. Haas, "On transmit diversity for spatial modulation MIMO: Impact of spatial constellation diagram and shaping filters at the transmitter," *IEEE Trans. Veh. Technol.*, vol. 62, no. 6, pp. 2507–2531, Jul. 2013.
[100] F. Oggier, "Cyclic algebras for noncoherent differential space–time coding," *IEEE Trans. Inf. Theory*, vol. 53, no. 9, pp. 3053–3065, Sep. 2007.
[101] S. Sugiura and L. Hanzo, "Effects of channel estimation on spatial modulation," *IEEE Signal Process. Lett.*, vol. 19, no. 12, pp. 805–808, Dec. 2012.
[102] N. Ishikawa and S. Sugiura, "Unified differential spatial modulation," *IEEE Wireless Commun. Lett.*, vol. 3, no. 4, pp. 337–340, Aug. 2014.
[103] M. Wen, Z. Ding, X. Cheng, Y. Bian, H. V. Poor, and B. Jiao, "Performance analysis of differential spatial modulation with two transmit antennas," *IEEE Commun. Lett.*, vol. 18, no. 3, pp. 475–478, Mar. 2014.
[104] Y. Bian, X. Cheng, M. Wen, L. Yang, H. V. Poor, and B. Jiao, "Differential spatial modulation," *IEEE Trans. Veh. Technol.*, vol. 64, no. 7, pp. 3262–3268, Jul. 2015.
[105] P. A. Martin, "Differential spatial modulation for APSK in time-varying fading channels," *IEEE Commun. Lett.*, vol. 19, no. 7, pp. 1261–1264, Jul. 2015.
[106] J. Li, M. Wen, X. Cheng, Y. Yan, S. Song, and M. H. Lee, "Differential spatial modulation with gray coded antenna activation order," *IEEE Commun. Lett.*, vol. 20, no. 6, pp. 1100–1103, Jun. 2016.
[107] R. Rajashekar, N. Ishikawa, S. Sugiura, K. V. S. Hari, and L. Hanzo, "Full-diversity dispersion matrices from algebraic field extensions for differential spatial modulation," *IEEE Trans. Veh. Technol.*, vol. 66, no. 1, pp. 385–394, Jan. 2017.
[108] A. G. Helmy, M. Di Renzo, and N. Al-Dhahir, "Differential spatially modulated space-time block codes with temporal permutations," *IEEE Trans. Veh. Technol.*, vol. 66, no. 8, pp. 7548–7552, Aug. 2017.
[109] R. Mesleh, S. Althunibat, and A. Younis, "Differential quadrature spatial modulation," *IEEE Trans. Commun.*, vol. 65, no. 9, pp. 3810–3817, Sep. 2017.
[110] E. Başar, Ü. Aygölü, E. Panayırcı, and H. V. Poor, "Orthogonal frequency division multiplexing with index modulation," *IEEE Trans. Signal Process.*, vol. 61, no. 22, pp. 5536–5549, Nov. 2013.
[111] R. Fan, Y. J. Yu, and Y. L. Guan, "Generalization of orthogonal frequency division multiplexing with index modulation," *IEEE Trans. Wireless Commun.*, vol. 14, no. 10, pp. 5350–5359, Oct. 2015.
[112] D. Tsonev, S. Sinanovic, and H. Haas, "Enhanced subcarrier index modulation (SIM) OFDM," in *Proc. IEEE GLOBECOM Workshops*, Houston, TX, USA, Dec. 2011, pp. 728–732.
[113] H. Ochiai and H. Imai, "On the distribution of the peak-to-average power ratio in OFDM signals," *IEEE Trans. Commun.*, vol. 49, no. 2, pp. 282–289, Feb. 2001.
[114] L. Hanzo, T. H. Liew, B. L. Yeap, R. Y. S. Tee, and S. X. Ng, *Turbo Coding, Turbo Equalisation and Space-Time Coding: For Transmission Over Fading Channels*. Hoboken, NJ, USA: Wiley, 2011.
[115] W. Ryan and S. Lin, *Channel Codes: Classical and Modern*. Cambridge, U.K.: Cambridge Univ. Press, 2009.
[116] N. Bonello, S. Chen, and L. Hanzo, "Low-density parity-check codes and their rateless relatives," *IEEE Commun. Surveys Tuts.*, vol. 13, no. 1, pp. 3–26, 1st Quart., 2011.
[117] R. M. Gagliardi, A. J. Mendez, M. R. Dale, and E. Park, "Fiber-optic digital video multiplexing using optical CDMA," *J. Lightw. Technol.*, vol. 11, no. 1, pp. 20–26, Jan. 1993.
[118] M. Z. Win and R. A. Scholtz, "Impulse radio: How it works," *IEEE Commun. Lett.*, vol. 2, no. 2, pp. 36–38, Feb. 1998.
[119] M. Z. Win and R. A. Scholtz, "Ultra-wide bandwidth time-hopping spread-spectrum impulse radio for wireless multiple-access communications," *IEEE Trans. Commun.*, vol. 48, no. 4, pp. 679–689, Apr. 2000.
[120] J. Choi, "Single-carrier index modulation and CS detection," in *Proc. IEEE Int. Conf. Commun.*, Paris, France, May 2017, pp. 1–6.
[121] J. Salz, "Optimum mean-square decision feedback equalization," *Bell Syst. Tech. J.*, vol. 52, no. 8, pp. 1341–1373, Oct. 1973.
[122] J. E. Mazo, "Faster-than-Nyquist signaling," *Bell Syst. Tech. J.*, vol. 54, no. 8, pp. 1451–1462, 1975.
[123] J. B. Anderson, F. Rusek, and V. Öwall, "Faster-than-Nyquist signaling," *Proc. IEEE*, vol. 101, no. 8, pp. 1817–1830, Aug. 2013.
[124] A. D. Liveris and C. N. Georghiades, "Exploiting faster-than-Nyquist signaling," *IEEE Trans. Commun.*, vol. 51, no. 9, pp. 1502–1511, Sep. 2003.
[125] A. Prlja and J. B. Anderson, "Reduced-complexity receivers for strongly narrowband intersymbol interference introduced by faster-than-Nyquist signaling," *IEEE Trans. Commun.*, vol. 60, no. 9, pp. 2591–2601, Sep. 2012.
[126] S. Sugiura, "Frequency-domain equalization of faster-than-Nyquist signaling," *IEEE Wireless Commun. Lett.*, vol. 2, no. 5, pp. 555–558, Oct. 2013.
[127] S. Sugiura and L. Hanzo, "Frequency-domain-equalization-aided iterative detection of faster-than-Nyquist signaling," *IEEE Trans. Veh. Technol.*, vol. 64, no. 5, pp. 2122–2128, May 2015.
[128] T. Ishihara and S. Sugiura, "Iterative frequency-domain joint channel estimation and data detection of faster-than-Nyquist signaling," *IEEE Trans. Wireless Commun.*, vol. 16, no. 9, pp. 6221–6231, Sep. 2017.
[129] M. Di Renzo, D. De Leonardis, F. Graziosi, and H. Haas, "Space shift keying (SSK–) MIMO with practical channel estimates," *IEEE Trans. Commun.*, vol. 60, no. 4, pp. 998–1012, Apr. 2012.
[130] E. Soujeri and G. Kaddoum, "The impact of antenna switching time on spatial modulation," *IEEE Wireless Commun. Lett.*, vol. 5, no. 3, pp. 256–259, Jun. 2016.
[131] L. Xiao, P. Yang, Y. Zhao, Y. Xiao, J. Liu, and S. Li, "Low-complexity tree search-based detection algorithms for generalized spatial modulation aided single carrier systems," in *Proc. IEEE Int. Conf. Commun.*, Kuala Lumpur, Malaysia, May 2016, pp. 1–6.
[132] L. He, J. Wang, and J. Song, "Information-aided iterative equalization: A novel approach for single-carrier spatial modulation in dispersive channels," *IEEE Trans. Veh. Technol.*, vol. 66, no. 5, pp. 4448–4452, May 2017.
[133] Y. Zhao, P. Yang, Y. Xiao, L. Xiao, B. Dong, and W. Xiang, "An improved frequency domain turbo equalizer for single-carrier spatial modulation systems," *IEEE Trans. Veh. Technol.*, vol. 66, no. 8, pp. 7568–7572, Aug. 2017.
[134] L. Xiao, Y. Xiao, P. Yang, J. Liu, S. Li, and W. Xiang, "Space-time block coded differential spatial modulation," *IEEE Trans. Veh. Technol.*, vol. 66, no. 10, pp. 8821–8834, Oct. 2017.

**SHINYA SUGIURA** (M'06–SM'12) received the B.S. and M.S. degrees in aeronautics and astronautics from Kyoto University, Kyoto, Japan, in 2002 and 2004, respectively, and the Ph.D. degree in electronics and electrical engineering from the University of Southampton, Southampton, U.K., in 2010.

From 2004 to 2012, he was a Research Scientist with Toyota Central Research and Development Laboratories, Inc., Aichi, Japan. Since 2013, he has been an Associate Professor with the Department of Computer and Information Sciences, Tokyo University of Agriculture and Technology, Tokyo, Japan, where he heads the Wireless Communications Research Group. His research has covered a range of areas in wireless communications, networking, signal processing, and antenna technology. He has authored or co-authored over 50 IEEE journal papers in these research fields.

Dr. Sugiura was a recipient of a number of awards, including the RIEC Award from the Foundation for the Promotion of Electrical Communication in 2016, the Young Scientists' Prize by the Minister of Education, Culture, Sports, Science and Technology of Japan in 2016, the 14th Funai Information Technology Award (First Prize) from the Funai Foundation in 2015, the 28th Telecom System Technology Award from the Telecommunications Advancement Foundation in 2013, the Sixth IEEE Communications Society Asia-Pacific Outstanding Young Researcher Award in 2011, the 13th Ericsson Young Scientist Award in 2011, and the 2008 IEEE Antennas and Propagation Society Japan Chapter Young Engineer Award. He was also certified as an Exemplary Reviewer of the IEEE COMMUNICATIONS LETTERS in 2013 and 2014.

**TAKUMI ISHIHARA** (S'16) received the B.E. and M.E. degrees in computer and information sciences from the Tokyo University of Agriculture and Technology, Tokyo, Japan, in 2016 and 2017, respectively, where he is currently pursuing the Ph.D. degree. His research interest is in faster-than-Nyquist signaling.

**MIYU NAKAO** (S'17) received the B.E. degree in computer and information sciences from the Tokyo University of Agriculture and Technology, Tokyo, Japan, in 2017, where she is currently pursuing the master's degree. Her research interest is in index modulation. She received the IEEE VTS Tokyo Chapter 2017 Young Researcher's Encouragement Award.